energies

MDPI

Review

Economic Analysis of Nuclear Energy Cogeneration: A Comprehensive Review on Integrated Utilization

Guobin Jia [1], Guifeng Zhu [1,2,*], Yang Zou [1,2,*], Yuwen Ma [1], Ye Dai [1,2], Jianhui Wu [1,2] and Jian Tian [1,2]

[1] Shanghai Institute of Applied Physics, Chinese Academy of Sciences, Shanghai 201800, China; jiaguobin@sinap.ac.cn (G.J.); mayuwen@sinap.ac.cn (Y.M.); daiye@sinap.ac.cn (Y.D.); wujianhui@sinap.ac.cn (J.W.); tianjian@sinap.ac.cn (J.T.)
[2] University of Chinese Academy of Sciences, Beijing 100049, China
* Correspondence: zhuguifeng@sinap.ac.cn (G.Z.); zouyang@sinap.ac.cn (Y.Z.)

Abstract: Nuclear energy cogeneration, which integrates electricity generation with thermal energy utilization, presents a transformative pathway for enhancing energy efficiency and decarbonizing industrial and urban sectors. This comprehensive review synthesizes advancements in technological stratification, economic modeling, and sectoral practices to evaluate the viability of nuclear cogeneration as a cornerstone of low-carbon energy transitions. By categorizing applications based on temperature requirements (low: <250 °C, medium: 250–550 °C, high: >550 °C), the study highlights the adaptability of reactor technologies, including light water reactors (LWRs), high-temperature gas-cooled reactors (HTGRs), and molten salt reactors (MSRs), to sector-specific demands. Key findings reveal that nuclear cogeneration systems achieve thermal efficiencies exceeding 80% in low-temperature applications and reduce CO_2 emissions by 1.5–2.5 million tons annually per reactor by displacing fossil fuel-based heat sources. Economic analyses emphasize the critical role of cost allocation methodologies, with exergy-based approaches reducing levelized costs by 18% in high-temperature applications. Policy instruments, such as carbon pricing, value-added tax (VAT) exemptions, and subsidized loans, enhance project viability, elevating net present values by 25–40% for district heating systems. Case studies from China, and Canada demonstrate operational successes, including 30% emission reductions in oil sands processing and hydrogen production costs as low as USD 3–5/kg via thermochemical cycles. Hybrid nuclear–renewable systems further stabilize energy supply, reducing the levelized cost of heat by 18%. The review underscores the necessity of integrating Generation IV reactors, thermal storage, and policy alignment to unlock nuclear cogeneration's full potential in achieving global decarbonization and energy security goals.

Keywords: nuclear cogeneration; economic analysis; reactor technologies; policy drivers; decarbonization

check for updates

Academic Editor: Massimo Dentice D'Accadia

Received: 12 May 2025
Revised: 27 May 2025
Accepted: 29 May 2025
Published: 3 June 2025
Corrected: 28 January 2026

Citation: Jia, G.; Zhu, G.; Zou, Y.; Ma, Y.; Dai, Y.; Wu, J.; Tian, J. Economic Analysis of Nuclear Energy Cogeneration: A Comprehensive Review on Integrated Utilization. *Energies* **2025**, *18*, 2929. https://doi.org/10.3390/en18112929

Copyright: © 2025 by the authors. Licensee MDPI, Basel, Switzerland. This article is an open access article distributed under the terms and conditions of the Creative Commons Attribution (CC BY) license (https://creativecommons.org/licenses/by/4.0/).

1. Introduction

Nuclear cogeneration refers to the simultaneous production of electricity and thermal energy for applications such as district heating, hydrogen production, or industrial process heat from a single nuclear reactor. Conventional nuclear power plants (NPPs), on the other hand, operate at thermal efficiencies of 30–35% and discharge approximately two-thirds of generated heat as waste through condenser cooling systems [1,2]. The discharge of waste heat from NPPs employing wet cooling systems constitutes a significant source of thermal pollution in aquatic ecosystems. These systems release heated effluents, typically 5–7 °C above ambient seawater temperatures, into coastal or riverine environments [3,4].

Elevated temperatures disrupt marine biodiversity by reducing dissolved oxygen levels, which alter metabolic rates in aquatic organisms [5]. Nuclear cogeneration systems recover and repurpose this waste heat, achieving overall efficiencies of 60–80% [1,6]. Recent work by Novotny et al. investigates nuclear–thermal energy storage configurations using high-temperature gas-cooled reactors (HTGRs). The thermodynamic analysis demonstrates that integrating thermal energy storage (TES) between the primary helium loop and the steam cycle improves flexibility and efficiency in industrial combined heat and power (CHP) systems. This approach avoids efficiency losses seen in traditional steam extraction methods and enables dynamic load-following capabilities [7].

The key applications include seawater [8–10], district heating [11,12], and industrial processes [13–15]. There are four advantages of nuclear cogeneration [16]: (1) Enhanced efficiency: By utilizing waste heat, cogeneration reduces primary energy waste, lowering operational costs and carbon intensity. (2) Economic viability: Synergies between electricity and heat production reduce per-unit energy costs. Studies suggest cogenerated heat from NPPs can be 30–50% cheaper than fossil-fuel alternatives [17]. (3) Decarbonization: Nuclear cogeneration eliminates ~1.5–2.5 million tons of CO_2 annually per reactor by displacing fossil fuel-based heat sources [17]. (4) Grid flexibility: Off-peak thermal energy production, such as hydrogen storage, enables load balancing, mitigating grid congestion and enhancing energy security [18]. Meanwhile, there are two driver forces for the development of nuclear cogeneration: (1) climate goals, aligning with the UN Sustainable Development Goals [19] and the Paris Agreement [20], and (2) energy security, which reduces reliance on imported fossil fuels, particularly for countries with limited grids or seasonal energy demand fluctuations [16].

Nuclear cogeneration systems can be categorized based on temperature requirements. For low-temperature applications (<250 °C), district heating and desalination are typical examples. Light water reactors (LWRs), such as pressurized water reactors (PWRs) and boiling water reactors (BWRs), dominate this space due to their mature steam extraction technologies [21]. On the other hand, high-temperature application scenarios (>550 °C) include hydrogen production and industrial process heat. These applications require advanced reactors like high temperature gas-cooled reactors (HTGRs) [22] or molten salt reactors (MSRs) [23], which are capable of delivering heat at temperatures ranging from 750 to 950 °C. For instance, Japan's GTHTR300C project has demonstrated that hydrogen production costs can be as low as USD 3–5/kg using thermochemical sulfur–iodine cycles [24]. The selection of reactor technology is critical to the feasibility of nuclear cogeneration. LWRs are well-suited for low-temperature applications, while Generation IV reactor designs, such as very-high-temperature reactors (VHTRs) [25], MSRs [26], and lead fast reactors [27], offer greater flexibility and high-temperature outputs, making them more suitable for emerging markets. The emergence of microreactors ($\leq$20 MWe) represents a paradigm shift in nuclear energy deployment, particularly for industrial CHP applications. These compact, factory-fabricated systems offer inherent safety features (e.g., passive cooling, TRISO fuel) and operational flexibility unmatched by traditional large-scale reactors. Microreactors like NuScale's VOYGR-SS (5–15 MWe) [28] and X-energy's Xe-100 (80 MWe) [29] are being designed with explicit consideration for industrial energy parks.

As of 2024, 79 reactors worldwide operate in cogeneration mode [30], primarily in Europe, Japan, and China. Key projects and their parameters are summarized in Table 1. As can be seen in Table 1, Russia leads in industrial-scale applications, with VVER-1200 [31] and BN-1200 [32] reactors supporting hydrogen and district heating. The BN-1200 fast reactor exemplifies high-temperature (750 °C) heat for thermochemical processes [33]. China's Haiyang [34] and Yanlong projects [35,36] highlight rapid deployment of SMR-based cogeneration, targeting urban heating and seawater desalination. Reactors oper-

ating in cogeneration mode encompass four types of reactors [16]. Specifically, there are 50 pressurized water reactors (PWRs) and boiling water reactors (BWRs), 9 pressurized heavy water reactors (PHWRs), 15 light water graphite reactors (LWGRs), and 1 sodium-cooled fast reactor (SFR).

Table 1. Existing and past operating nuclear cogeneration reactor parameters [7,29].

Country and Plant	Reactor Type	Net Capacity [MWe]	Thermal Capacity [MWth]	Temperature/Pressure	Remarks
Desalination					
Japan, Ohi-1,2	PWR	2 × 1175	2 × 3120	130 °C/0.3 MPa	MSF (1 × 1300 m^3/d), MED (2 × 1300 m^3/d)
Japan, Ohi-3,4	PWR	2 × 1180	2 × 3415	150 °C/0.4 MPa	RO (1 × 1300 m^3/d)
Kazakhstan, BN-350 (Aktau)	LMFR	150	750	150 °C/0.5 MPa	Largest nuclear desalination plant; MED & MSF
India, Kalpakkam-1,2	PHWR	235	760	120 °C/0.25 MPa	Hybrid MSF/RO
Saudi Arabia, KA-CARE (planned)	HTGR	2 × 105	2 × 450	250 °C/6.0 MPa	High-temperature MED-TVC feasibility study
District heating					
Russia, Novovoronezh-3,4	VVER-440	2 × 385	2 × 1375	130 °C/0.8 MPa	50 km pipeline network
China, Haiyang-1,2	PWR	2 × 1000	2 × 3415	130 °C/1.5 MPa	23 km pipeline; integrated with urban heating
Czech Republic, Temelin-1,2	VVER-1000	2 × 1086	2 × 3120	150 °C/1.0 MPa	5 km & 26 km dual pipelines
Switzerland, Beznau-1,2	PWR	365, 357	2 × 1130	128 °C/0.7 MPa	35 km pipeline; seasonal load management
Slovakia, Bohunice-3,4	VVER-440	2 × 365	2 ×1471	150 °C/1.2 MPa	18 km pipeline; peak demand via HP extraction
Process heat					
Canada, Bruce A	PHWR	811, 777	2 × 2620	190 °C/1.8 MPa	Heavy water production; Bruce Energy Centre
Germany, Stade	PWR	640	1900	190 °C/1.5 MPa	Salt refinery integration
Norway, Halden (experimental)	BWR	-	35	240 °C/3.4 MPa	Intermittent operation for pulp/paper plant
China, Tianwan-1,2	PWR (VVER-1000)	2 × 1000	2 × 3000	248 °C/1.8 MPa	Refinery and chemical plants; 23 km steam pipeline
Romania, Cernavoda-1	PHWR (CANDU-6)	660	2180	150 °C/0.6 MPa	2 km pipeline; low-temperature process heat
Advanced reactors (R&D)					
USA, Xe-100 (demonstration)	HTGR (Xe-100)	80	200	750 °C/7.0 MPa	Flexible CHP with molten-salt TES; hydrogen co-production
Russia, BN-800	LMFR	789	2100	500 °C/14.0 MPa	High-temperature process heat for petrochemicals
South Korea, SMART	PWR	100	330	250 °C/4.2 MPa	SMR-based desalination and district heating
France, Astrid (canceled)	Sodium-cooled fast reactor	600	1500	550 °C/18.0 MPa	Planned for industrial heat; canceled in 2019
UK, U-Battery (concept)	HTGR (microreactor)	4	10	750 °C/5.0 MPa	Modular design for decentralized industrial parks
Historical Projects					
USSR, Beloyarsk-3	LMFR (BN-600)	560	1470	500 °C/10.0 MPa	Pioneering nuclear process heat for aluminum production (1980–2015)

Table 1. *Cont.*

Country and Plant	Reactor Type	Net Capacity [MWe]	Thermal Capacity [MWth]	Temperature/Pressure	Remarks
East Germany, Rheinsberg	PWR (VVER-70)	70	265	200 °C/1.0 MPa	District heating until 1990
Canada, Gentilly-2	HWR (CANDU-6)	675	2100	180 °C/1.2 MPa	Heavy water and isotope production (1983–2012)
Emerging SMRs					
USA, NuScale VOYGR	PWR	77 × 12	250 × 12	300 °C/8.0 MPa	Multi-module desalination and hydrogen production
Argentina, CAREM-25	PWR	25	100	220 °C/3.5 MPa	Compact design for remote industrial complexes
Russia, RITM-200	PWR	175	500	300 °C/6.0 MPa	Arctic industrial heat and power solutions

District heating represents a prospective pathway for nuclear cogeneration, and current research emphasizes the technical feasibility of integrating nuclear power plants (NPPs) with district heating networks through low-temperature steam extraction or secondary-circuit heat exchange [15,37]. For instance, Sweden's feasibility studies propose coupling NPP waste heat with building thermal energy storage (TES) systems to address intermittency challenges in urban heating, achieving theoretical energy efficiency gains of 12–18% compared to standalone power generation [38]. Notable operational examples include China's Haiyang NPP Phase I, which delivers 2.5×10^5 GJ annually for space heating via secondary-circuit modifications, reducing coal consumption by 23,000 metric tons/year [34]. Economic analyses indicate marginal competitiveness without government subsidies, highlighting dependency on carbon pricing mechanisms.

Industrial heat applications are also gaining traction, such as Canada's oil sands processing [39], which can reduce CO_2 emissions by 30% through 250 °C steam supplied by small modular reactors, and China's integration of HPR1000 with petrochemical sectors [40]. Furthermore, nuclear–renewable hybrid energy systems are emerging as a way to optimize economics through thermal storage and multi-energy synergies [18,41], as shown in Figure 1 [7]. Figure 1a illustrates a steam extraction-based thermal energy storage (TES) integration, where steam is diverted from the main steam line to charge the TES system. This configuration could considerably increase costs due to the very high pressure requirements on the storage vessel, with limited flexibility in balancing heat-to-power ratios. In contrast, Figure 1b demonstrates TES integration via the reactor's primary helium loop using an intermediate heat exchanger. This approach decouples the nuclear heat source from the power cycle, enabling independent control of heat dispatch to storage, electricity generation, and process steam supply. This configuration achieves greater operational flexibility while maintaining reactor stability during load transients.

Key economic evaluation metrics include the levelized cost of electricity (LCOE), levelized cost of non-electricity (LCONE), net present value (NPV), and internal rate of return (IRR). These tools enable cross-comparisons between nuclear cogeneration and alternative decarbonization pathways, such as fossil-based systems with carbon capture or renewable hybrids. Recent studies emphasize the role of carbon pricing in improving NPV by 25–40% for district heating projects [30,42] and the impact of policy incentives, such as tax credits for hydrogen production [43], in bridging cost gaps with fossil competitors. Meanwhile, the economic assessments of nuclear cogeneration require sophisticated frameworks to address cost allocation challenges and multi-product revenue streams. Two primary methodologies dominate: (1) energy-equivalent methods, which attribute thermal costs to equivalent electricity losses, and (2) exergy-based approaches, which optimize energy quality allocation using second-law thermodynamics [17].

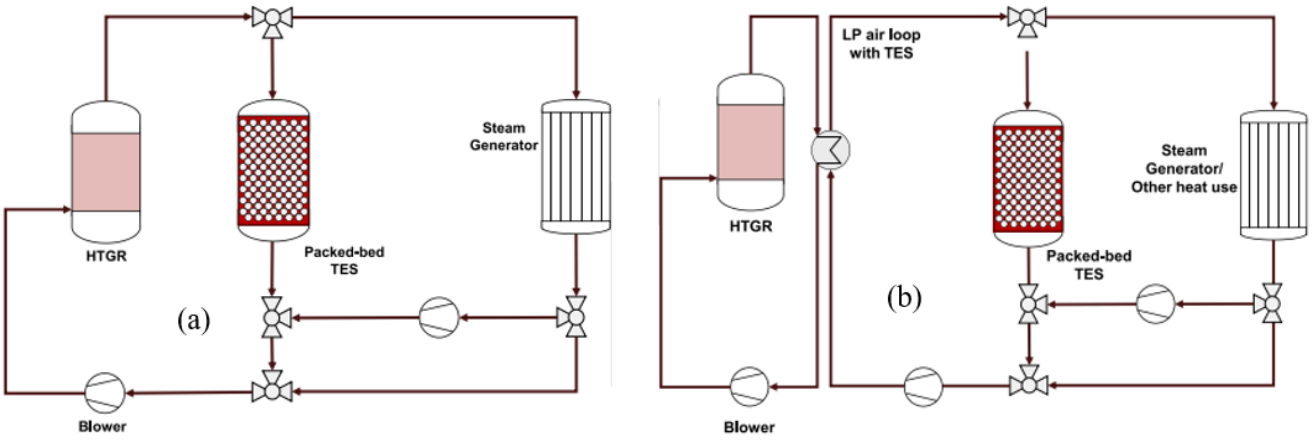

Figure 1. Two conceptual integrated energy system layouts that integrate a high-temperature gas-cooled reactor with packed-bed thermal energy storage: (**a**) TES integrated into the primary helium loop, and (**b**) TES with an intermediate low-pressure air loop [7].

Existing studies on nuclear cogeneration often focus narrowly on technical feasibility or economic modeling, with limited integration of policy and market dynamics. This review addresses critical gaps by synthesizing advancements across three dimensions: (1) technological stratification: categorizing applications by temperature requirements and reactor compatibility to identify optimal system configurations; (2) economic viability: evaluating cost allocation frameworks, hybrid energy systems, and policy-driven financial mechanisms; and (3) sectoral practices: analyzing regional case studies and market trends to derive actionable insights for stakeholders. By bridging these interdisciplinary perspectives, this work aims to accelerate the adoption of nuclear cogeneration as a cornerstone of global decarbonization strategies. The paper is organized as follows: Section 2 provides an overview of the technical landscape of nuclear cogeneration. Sections 3 and 4 delve into economic frameworks and present sectoral case studies. Section 5 examines market dynamics and policy drivers. Section 6 provides the future prospect for nuclear cogeneration. Finally, Section 7 presents the conclusions of the review.

2. Technical Landscape of Nuclear Cogeneration

2.1. Classification of Nuclear Cogeneration Applications

Nuclear cogeneration systems exhibit temperature-dependent specialization, with three distinct application tiers, as shown in Table 2.

Table 2. Classification of nuclear cogeneration applications by thermal range.

Thermal Range	Applications	Reactor Types	Case
<250 °C	District heating, RO desalination	PWR, BWR	China Haiyang [34]
250–550 °C	MED desalination, petrochemicals	CANDU, PHWR	Canada SMR [44]
>550 °C	HT electrolysis, steel production	HTGR, MSR, VHTR	Japan GTHTR300C [24], China HTR-PM [45]

2.1.1. Low-Temperature Applications (<250 °C)

District heating has been successfully implemented in China's Haiyang low-temperature reactor [34]. These systems achieve remarkable thermal efficiencies by integrating steam bypass systems with hot water networks. Notably, China's Haiyang NPP demonstrates a breakthrough with 4.5 million m^2 heating coverage via 120 °C steam extraction, achieving a 72.5% annual load factor while maintaining baseload power.

In the context of desalination, pairing reverse osmosis (RO) and multi-effect distillation (MED) systems with light water reactors enables the production of 50,000–120,000 m^3/day of freshwater. Saudi Arabia's proposed nuclear–RO plants are a prime example [46,47], achieving competitive levelized water costs of USD 0.8–1.2/m^3, which are on par with fossil-based desalination systems.

2.1.2. Medium-Temperature System (250–550 °C)

Medium-temperature nuclear cogeneration systems, operating within the 250–550 °C range, are gaining prominence in decarbonizing energy-intensive petrochemical processes by displacing fossil-derived steam while enhancing operational reliability. In Canada's oil sands sector, the small modular reactor (SMR) delivers 280 °C saturated steam at 6.4 MPa for bitumen extraction via steam-assisted gravity drainage [48,49]. This application has reduced process-level carbon intensity from 68 to 48 kg of CO_2 per barrel, primarily by eliminating natural gas combustion for steam generation. In China, the HTR-PM high-temperature reactor supplies 540 °C superheated steam at 13.8 MPa to methanol synthesis reactors, achieving dual benefits: a 22% improvement in thermochemical conversion efficiency compared to conventional natural gas-fired systems, and a 1.8-fold extension in catalyst service life due to reduced thermal cycling and impurity ingress [45]. These case studies demonstrate the capacity of medium-temperature nuclear cogeneration to simultaneously address emissions reduction and process optimization in hydrocarbon processing industries.

2.1.3. High-Temperature Applications (>550 °C)

High-temperature nuclear cogeneration demonstrates significant potential in advancing cost-competitive, low-carbon hydrogen production. Japan's GTHTR300C project has validated the commercial viability of thermochemical sulfur–iodine (S-I) cycles [50,51], utilizing 850 °C process heat from high-temperature gas-cooled reactors (HTGRs). This system achieves hydrogen production costs of USD 3–5 per kilogram, representing a 40% reduction compared to conventional proton-exchange membrane electrolysis, primarily due to the elimination of electricity-intensive water-splitting stages. The integration of nuclear heat with thermochemical processes bypasses the Carnot efficiency limitations inherent in power-to-hydrogen pathways, positioning HTGR-driven S-I cycles as a scalable solution for industrial hydrogen demand.

High-temperature nuclear cogeneration also enables the decarbonization of energy-intensive industrial processes through the provision of 750 °C steam, adaptable to sector-specific thermal requirements.

2.2. Reactor Technologies for Cogeneration

Table 3 is a comparative table of nuclear reactor types for cogeneration, including an LWGR (light water graphite reactor, e.g., RBMK) and a PHWR (pressurized heavy water reactor, e.g., CANDU), alongside some Generation IV reactors.

Table 3. Comparative analysis of nuclear reactor types for cogeneration.

Reactor Type	Thermal Efficiency (%)	Temperature Range	Advantage	Disadvantage
PWR (pressurized water reactor) [52,53]	33–35	280–320	Mature technology, high operational reliability	Limited temperature for industrial heat
BWR (boiling water reactor) [54]	32–34	285–315	Simplified design, direct steam cycle	Lower thermal efficiency, limited scalability

Table 3. *Cont.*

Reactor Type	Thermal Efficiency (%)	Temperature Range	Advantage	Disadvantage
PHWR (CANDU) [55]	29–30	250–300	Natural uranium fuel, high neutron economy	Lower thermal efficiency, high heavy water costs
LWGR (RBMK) [56]	28–30	250–280	Enhanced neutron economy	Safety concerns, low thermal efficiency
HTGR (high-temperature gas-cooled reactor) [22]	40–50	700–950	High-temperature output, inherent safety	High capital costs, limited large-scale deployment
MSR (molten salt reactor) [57]	45–50	700–1000	Fuel flexibility, passive safety	Corrosion challenges, low TRL

2.2.1. Light Water Reactors

Light water reactors include pressurized water reactors (PWRs) and boiling water reactors (BWRs). PWRs and BWRs are mature technologies but are limited to low-temperature applications. For instance, retrofitted PWRs can extract 10–15% of thermal power through secondary loops for district heating purposes, all while maintaining baseload electricity output [21], as shown in Figure 2.

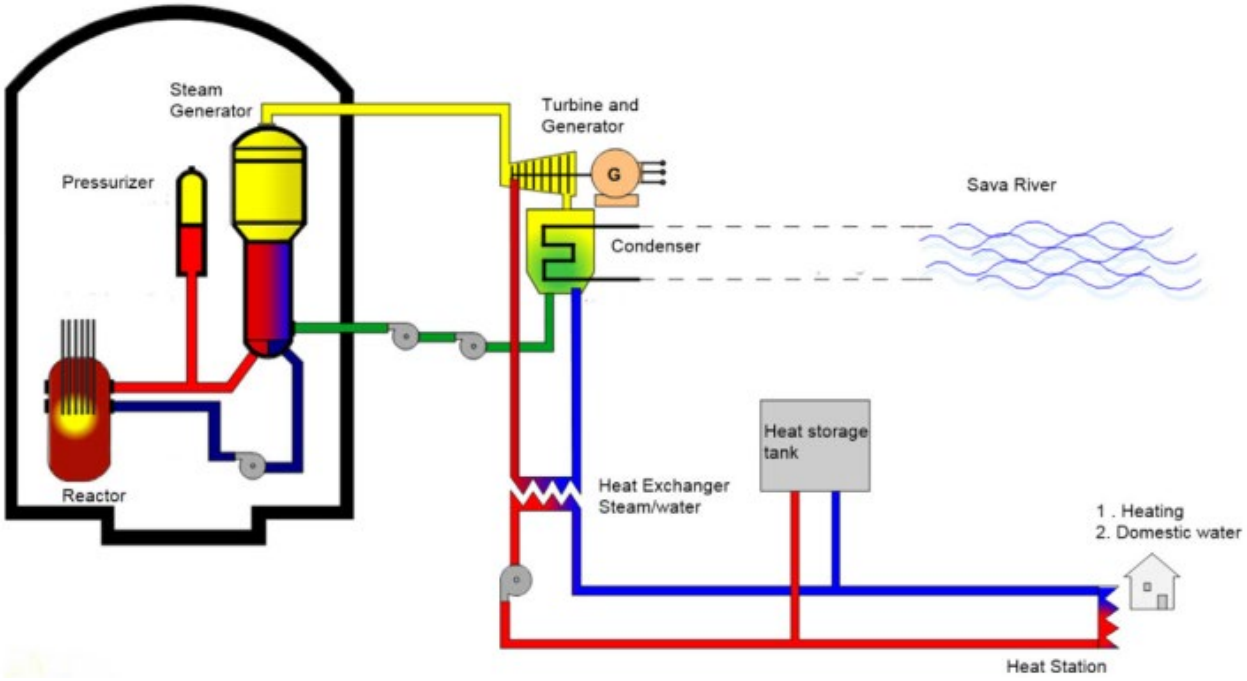

Figure 2. Schematic of district heating integration with a pressurized water reactor-based CHP [17]. Adapted from source: OECD/NEA (2024), Beyond Electricity: The Economics of Nuclear Cogeneration, https://www.oecd-nea.org/jcms/pl_71699/beyond-electricity-the-economics-of-nuclear-cogeneration?details=true (accessed on 28 May 2025), with source attribution under non-commercial terms.

Advanced LWRs have incorporated passive safety features and modular designs. NuScale integrates thermal energy storage (TES) to accommodate thermal extraction [28,58]. This allows for flexible heat-to-power ratios ranging from 0.5 to 1.5, making it highly suitable for industrial parks.

2.2.2. Light Water Graphite Reactor

A light water graphite reactor (LWGR) employs graphite blocks as the neutron moderator and light water (H_2O) as the coolant, with uranium dioxide (UO_2) as the primary fuel [59], as shown in Figure 3. Modern LWGRs integrate passive safety systems, such as emergency core cooling and negative temperature reactivity coefficients, addressing

historical flaws like the positive void coefficient in early RBMK designs. LWGRs can supply low- to medium-temperature heat (150–300 °C), suitable for district heating, seawater desalination, or industrial processes [60].

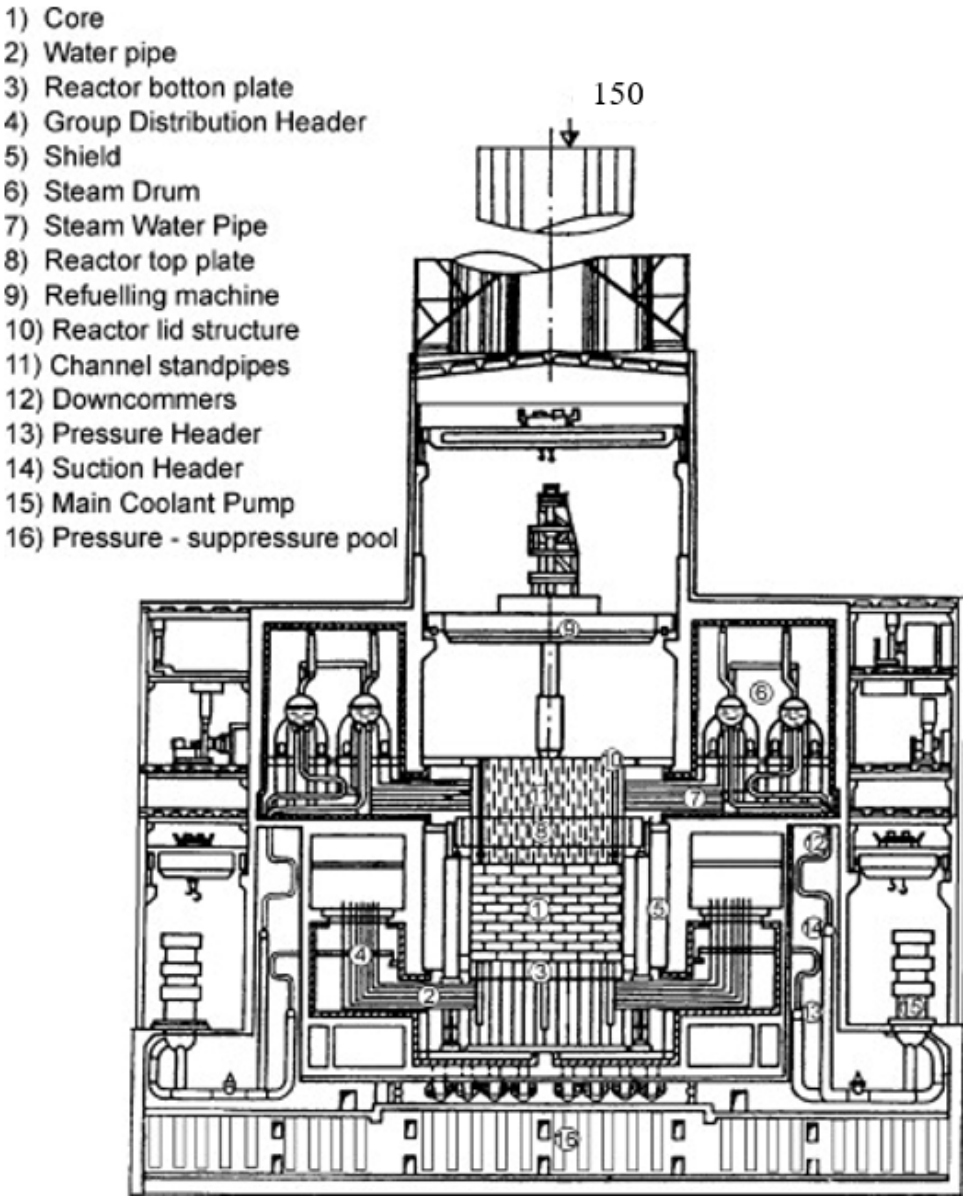

Figure 3. Sketch of the main coolant circuit of an RBMK [56].

2.2.3. Pressurized Heavy Water Reactors

Pressurized heavy water reactors (PHWRs) [55], exemplified by the CANDU (Canada Deuterium Uranium) design, utilize heavy water (D_2O) as both moderator and coolant, enabling the use of natural uranium fuel due to superior neutron economy, as shown in Figure 4. This reactor type operates at high pressures (~10 MPa) to maintain coolant temperatures below boiling, with core outlet temperatures typically ranging between 250 °C and 310 °C. The modular fuel channel design allows for online refueling, ensuring continuous operation and high-capacity factors (>85%). PHWRs are inherently suited for nuclear cogeneration—the simultaneous production of electricity and process heat—due to their thermal output flexibility, fuel efficiency, and compatibility with industrial heat requirements.

A key advantage of PHWRs in cogeneration lies in their ability to deliver high-temperature steam or hot water for industrial applications. The Madras Atomic Power Station at Kalpakkam [61] utilizes a hybrid desalination system. It combines Multi-Stage Flash (MSF) distillation and Reverse Osmosis (RO) technologies. With a total capacity of 6300 m^3/day, the plant produces high-purity water for reactor and domestic use.

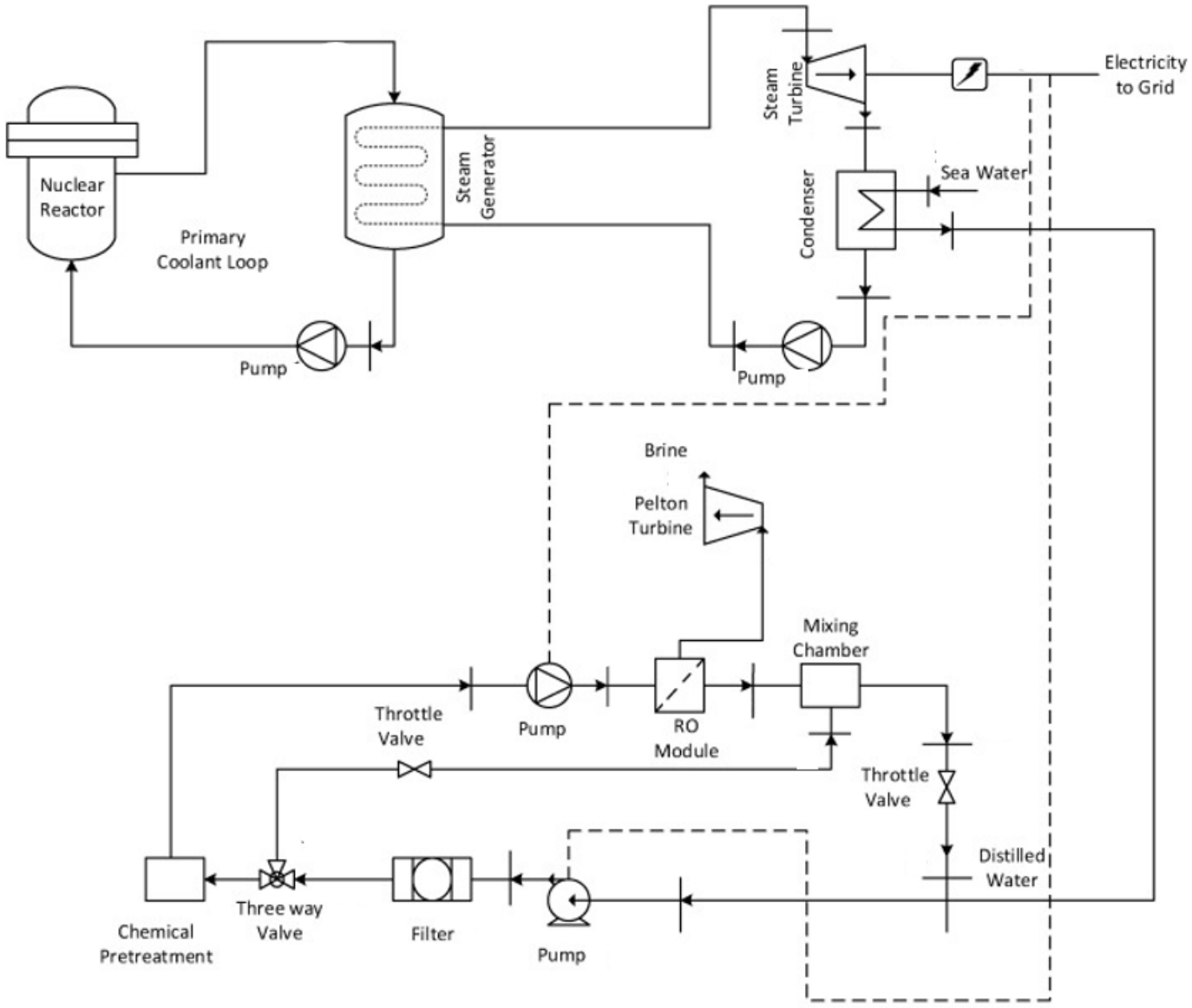

Figure 4. CANDU reactor configuration for seawater desalination [62].

2.2.4. Advanced Reactors

The core outlet temperatures of high-temperature gas-cooled reactors (HTGRs) is 750–950 °C, enabling applications such as thermochemical hydrogen production and industrial process heat supply, as shown in Figure 5. The next-generation nuclear plant project has validated a 50% efficiency in hydrogen coproduction using helium-cooled prismatic cores [63].

Molten salt reactors (MSRs) offer another advanced option [64]. Liquid-fueled MSRs, such as Terrestrial Energy's IMSR, operate at 700 °C and feature inherent load-following capabilities. Dual-fluid MSRs can achieve an impressive 85% exergy efficiency by directly coupling heat exchangers to chemical plants [26].

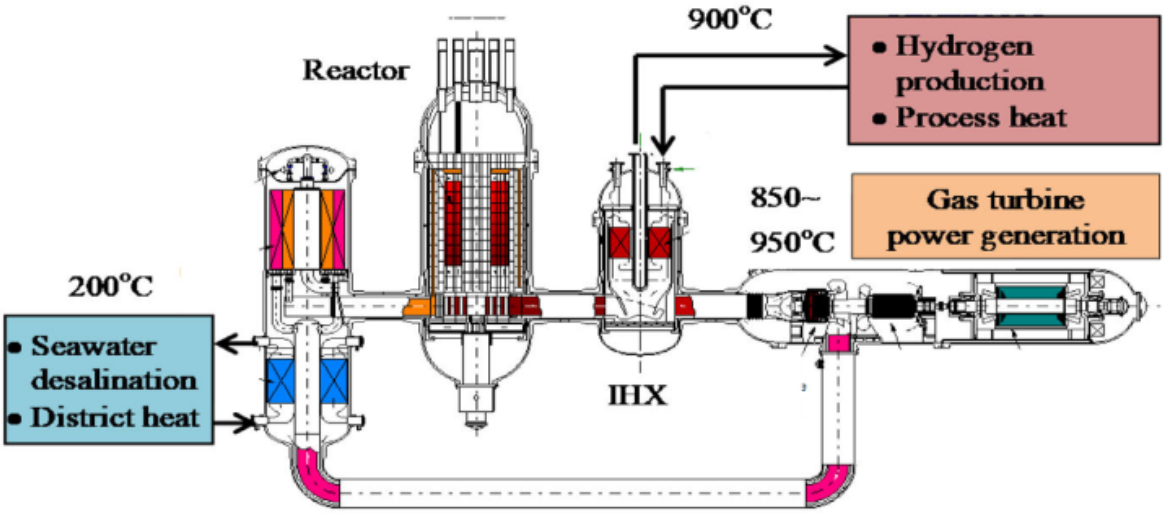

Figure 5. GTHTR300C for power generation with various cogeneration options [17]. Adapted from source: OECD/NEA (2024), Beyond Electricity: The Economics of Nuclear Cogeneration, https://www.oecd-nea.org/jcms/pl_71699/beyond-electricity-the-economics-of-nuclear-cogeneration?details=true (accessed on 28 May 2025), with source attribution under non-commercial terms.

2.3. Integration Methodologies

2.3.1. Thermal Extraction Techniques

Steam bypass is a technique commonly employed in LWR retrofits. It diverts 5–20% of steam to district heating networks. However, this process does lead to a reduction in electricity output of 8–12%. Secondary loops are utilized in HTGRs, which employ intermediate heat exchangers to isolate nuclear and industrial circuits. The GTHTR300C's helium-to-steam IHX is a prime example [24]. It minimizes contamination risks while maintaining an 88% thermal transfer efficiency.

2.3.2. Coupling with Thermal Energy Storage

Thermal energy storage (TES) effectively decouples heat production from heat demand, thereby enhancing system flexibility. There are three types of thermal energy storage [65]: (1) sensible heat storage systems, such as two tank molten salt systems paired with HTGRs, which can buffer 500 MWhth at 565 °C; (2) latent heat storage, which utilizes phase change materials (PCMs) to store heat in the 200–400 °C range and has proven particularly effective for MED desalination, doubling the daily water output in pilot projects in the UAE [66]; and (3) hybrid TES configurations, such as integrated energy systems [41], which combine nuclear, solar thermal, and rock-bed TES.

3. Economic Models for Nuclear Cogeneration

3.1. Economic Evaluation Models

Economic models quantify the financial viability of nuclear cogeneration systems by balancing capital investments, operational costs, and revenue streams. The economic evaluation of dual-purpose cogeneration systems is conducted through a comparative framework that benchmarks performance against a reference single-purpose power plant. The detailed flowchart is shown in Figure 6. First, the net energy output and total expenses of the standalone power plant are calculated, enabling derivation of the cost per saleable kilowatt-hour. Subsequently, the dual-purpose plant's parameters are quantified, including its reduced net saleable electricity output, production of cogeneration, and elevated total expenses. Finally, the levelized cost of non-electric product is calculated.

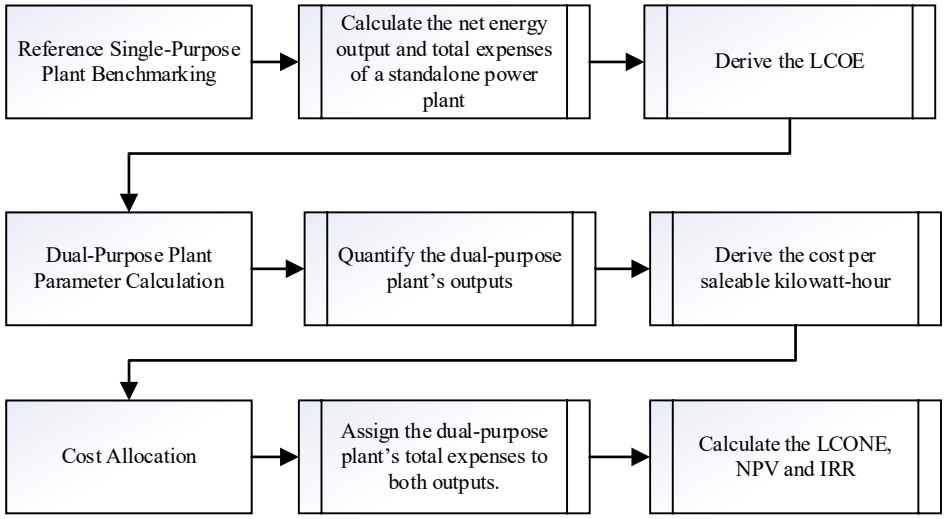

Figure 6. Flowchart of economic evaluation for nuclear cogeneration.

3.1.1. LCOE Model

This section evaluates LCOE models that explicitly or implicitly address temporal effects in nuclear economics, and the comparison is shown in Table 4.

Table 4. Comparison of different LCOE models.

Model	Time Handling	Strengths	Weaknesses
IAEA standard [17]	Full discounting	Benchmarking; lifecycle transparency	Overreliance on discount rate; ignores fuel-phase links
Static (Gen-IV) [67]	No discounting on O&M or fuel cost	Simplicity; rapid scenario testing	Misleading for long-term projects on operational cost and fuel cost
Monte Carlo [68]	Probabilistic discounting	Risk quantification; endogenous correlations	Computational cost; expert dependency

(1) Standard LCOE with Time Discounting

Adopted by IAEA and OECD/NEA [16,30], this model integrates time-value adjustments for lifecycle costs and energy outputs.

$$LCOE = \frac{\sum_{t=0}^{T} \frac{I_t + M_t + F_t + D_t}{(1+r)^t}}{\sum_{t=0}^{T} \frac{E_t}{(1+r)^t}} \quad (1)$$

where I_t represents the capital expenditure (the cost of overnight and financing) at year t; M_t, F_t, and D_t are the operational and maintenance costs, fuel cycle costs, and decommissioning costs at year t, respectively; E_t is the annual electricity output; and r is the discount rate.

(2) Static LCOE

Used in G4ECONS analyses [67], this omits discounting for operational phases, focusing on annualized averages.

$$LCOE = \frac{TCIC \times CRF + AOM + DC \times SFF}{E} + LUFEC + LUBEC \quad (2)$$

where AOM represents the average annual operation and maintenance costs, DC is the decommissioning costs, and $TCIC$ is the total construction cost, which includes overnight

capital costs, financing costs, and the first core fuel load costs. The capital recovery factor (CRF) and sinking fund factor (SFF) are calculated as follows:

$$CRF = \frac{i(1+i)^L}{\left[(1+i)^L - 1\right]} \tag{3}$$

$$SFF = \frac{i}{(1+i)^L - 1} \tag{4}$$

where i is the annual interest rate, and L is the plant lifetime in years.

In Equation (2), E represents the average annual electricity generation of the nuclear power plant in MWh, calculated as shown below:

$$E = P_E \times 365 \times 24 \times F_{capacity} \tag{5}$$

where P_E is the electrical power of the nuclear power plant, and $F_{capacity}$ represents the capacity factor of the nuclear power plant, which is the proportion of time in a year that the nuclear power plant operates at full capacity.

The formulas for calculating the LCOE of the front-end fuel cycle (LUFEC) and back-end fuel cycle (LUBEC) are as follows:

$$LUFEC = \frac{\sum_i m_i U_i}{\sum_k E_k} \tag{6}$$

$$LUBEC = \frac{\sum_i m_i U_i}{\sum_k E_k} \tag{7}$$

In Formulas (6) and (7), the subscript i indicates the ith step in the fuel cycle, the subscript k indicates the kth year in the lifespan, m_i represents the mass of heavy metal processed in the ith step, and in the enrichment power calculation. U_i represents the cost of processing one unit of heavy metal in the ith stage, and E_k represents the electricity generation in the kth year.

(3) Monte Carlo LCOE with Endogenous Risks

In order to quantify uncertainty bands and identify dominant risk drivers, Ref. [68] incorporates stochastic variables (construction delays, interest rates) via probabilistic simulations, which can be calculated as:

$$LCOE_{MC} = \mathrm{E}\left[\frac{\sum_{t=0}^{T} \frac{I_t(\omega)+M_t(\omega)+F_t(\omega)+D_t}{(1+r(\omega))^t}}{\sum_{t=0}^{T} \frac{E_t(\omega)}{(1+r(\omega))^t}}\right] \tag{8}$$

where ω is a stochastic weighting factor representing the probability distribution of uncertain variables in the Monte Carlo simulation.

3.1.2. Levelized Cost of Non-Electricity Model

The operational and economic parameters of the dual-purpose cogeneration plant are systematically quantified. The net saleable electricity output (E_{cogen}) is reduced compared to the reference single-purpose plant ($E_{cogen} < E_{ref}$) due to thermal energy allocation for district heating, desalination, or hydrogen production. Concurrently, the total expenses (C_{cogen}) increase relative to the standalone plant ($C_{cogen} > C_{ref}$) owing to additional capital

and operational costs associated with cogeneration infrastructure. For the non-electric output W_{prod}, the levelized cost of the non-electric product (LCONE) is calculated as:

$$LCONE = \frac{C_{cogen} - E_{cogen} \times LCOE}{W_{prod}} \quad (9)$$

where LCOE represent the levelized cost of electricity.

3.1.3. Profitability Indicators

Profitability indicators are critical for assessing the financial viability of nuclear cogeneration projects. Two widely used metrics, net present value (NPV) and internal rate of return (IRR), are essential for comparing investment options and evaluating long-term economic feasibility.

NPV quantifies the difference between the present value of cash inflows (revenues) and outflows (costs) over the project lifetime. A positive NPV indicates profitability [69], which can be calculated as:

$$NPV = \sum_{t=0}^{N} \frac{C_{in,t} - C_{out,t}}{(1+r)^t} - C_{initial} \quad (10)$$

where $C_{in,t}$ and $C_{out,t}$ represent cash inflows and outflow in year t, r is the discount rate, and $C_{initial}$ is the initial capital expenditure. N is the project lifetime (years).

IRR is the discount rate at which the NPV equals zero. It represents the project's expected annualized return [70]. The formula is as follows:

$$\sum_{t=0}^{N} \frac{C_{in,t} - C_{out,t}}{(1+IRR)^t} - C_{initial} = 0 \quad (11)$$

NPV and IRR complement levelized cost metrics by incorporating temporal cash flow dynamics.

Nuclear cogeneration (NCG) integrates electricity generation with thermal energy utilization for district heating, industrial processes, or hydrogen production. This section reviews theoretical frameworks and mathematical models employed in NCG system analysis, categorized into four domains: thermodynamic modeling, economic evaluation, hybrid system optimization, and cost allocation methodologies.

3.2. Cost Allocation

Cost allocation in nuclear cogeneration (NCG) systems is a critical process for equitably distributing joint operational and capital costs between electricity and thermal energy outputs, such as district heating, industrial process steam, or hydrogen production. This methodology ensures transparent pricing, informs subsidy design, and enables accurate benchmarking against fossil fuel-based alternatives. The complexity arises from the shared infrastructure and interdependent production processes, necessitating frameworks that balance thermodynamic principles, market dynamics, and regulatory requirements. Four primary methodologies dominate cost allocation in NCG systems [17]: energy-based [71], exergy-based [71,72], opportunity cost [73], and proportional benefit approaches [17], each of which has distinct mathematical formulations and contextual applicability, and the comparison is shown in Table 5.

Table 5. Comparison of cost allocation methodologies in nuclear cogeneration.

Method	Basis	Strengths	Weaknesses	Typical Applications
Energy credit [71]	Energy quantity (enthalpy)	Simplicity; regulatory compliance	Ignores energy quality; undervalues high-T heat	District heating
Exergy-based [72]	Thermodynamic work potential	Reflects energy grade; technical rigor	Data-intensive; limited policy adoption	High-temperature hydrogen
Opportunity cost [73]	Foregone electricity revenue	Market-aligned; flexible for retrofits	Volatility in electricity prices	Retrofitted PWRs
Proportional benefit [17]	Revenue share	Aligns with economic value; market-responsive	Requires stable revenue data	Deregulated markets

3.2.1. Energy Credit Method

The overall energy efficiency of a cogeneration system is expressed as:

$$\eta_{en} = \frac{W_{el} + Q_{proc}}{Q_{th}} \tag{12}$$

where W_{el} is the electrical output, Q_{proc} represents the usable process heat, and Q_{th} denotes the total thermal energy generated by the reactor. This metric, however, overlooks the quality of thermal energy, necessitating exergy-based assessments.

The energy credit method allocates costs proportionally to the energy content of each output, measured in terms of enthalpy. This approach calculates the cost share for thermal energy (C_{proc}) and electricity (C_{el}) using the ratio of their respective energy outputs to the total system output:

$$C_{prod} = C_{total} \frac{Q_{proc}}{W_{el} + Q_{proc}} \tag{13}$$

$$C_{el} = C_{total} \frac{W_{el}}{W_{el} + Q_{proc}} \tag{14}$$

where C_{total} represents the total system cost, Q_{proc} is the thermal energy output (MWh), and W_{el} is the electrical energy output (MWh). While straightforward and widely adopted in district heating projects, this method overlooks the thermodynamic quality of heat.

3.2.2. Exergy-Based Method

While the energy credit method is straightforward and widely adopted in district heating projects, this method overlooks the thermodynamic quality of heat. To address this limitation, the exergy-based allocation method incorporates the thermodynamic work potential, which is the exergy, of energy streams. Exergy quantifies the usable energy fraction, factoring in temperature and ambient conditions.

$$\eta_{ex} = \frac{W_{el} + \psi_{proc}}{Ex_{th}} \tag{15}$$

where Ex_{th} is the total exergy input from the reactor, and ψ_{proc} represents the exergy of process heat at temperature, which can be calculated as:

$$\psi_{proc} = Q_{proc}\left(1 - \frac{T_0}{T_{proc}}\right) \tag{16}$$

where T_{proc} is the heat delivery temperature (K), and T_0 is ambient temperature. Exergy destruction in heat exchangers and turbines often constitutes the largest loss component, particularly in high-temperature applications like hydrogen production via thermochemical cycles.

The cost allocation formula can be expressed as:

$$C_{prod} = C_{total} \frac{\psi_{proc}}{\psi_{proc} + W_{el}} \tag{17}$$

where ψ_{proc} is the exergy of process heat. This method is particularly relevant for high-temperature applications.

3.2.3. Opportunity Cost Approach

The opportunity cost approach values thermal energy based on the revenue foregone from reduced electricity generation. This method calculates the cost of heat production as the difference between the revenue generated in a standalone power plant and a cogeneration system.

$$C_{prod} = \frac{C_{total} - \left(W_{el}^{base} \cdot p_{el}\right)}{\eta_{th} Q_{proc}} \tag{18}$$

where W_{el}^{base} is the electricity output of a power-only plant, p_{el} is the electricity price, and η_{th} is the thermal efficiency penalty from heat extraction.

3.2.4. Proportional Benefit Method

The proportional benefit method allocates costs based on the revenue share of each product, aligning with market-driven pricing strategies. The formulas are:

$$C_{proc} = C_{total} \frac{R_{proc}}{R_{proc} + R_{el}} \tag{19}$$

$$C_{proc} = C_{total} \frac{R_{el}}{R_{proc} + R_{el}} \tag{20}$$

where R_{proc} and R_{el} represent revenue from thermal energy and electricity sales, respectively. This approach is effective in deregulated markets, where nuclear plants supplying process heat to chemical industries price outputs based on real-time market value. However, it requires stable revenue streams and is less applicable to non-commercial or subsidized projects.

3.3. Policy-Driven Economics

Policy instruments critically determine the economic viability of nuclear cogeneration by reshaping cost–benefit equilibria across energy markets. Carbon pricing mechanisms, value-added tax (VAT) exemptions for non-electric outputs, and subsidized long-term loans collectively alter net present value (NPV) dynamics, as evidenced by cross-country analyses from the OECD Nuclear Energy Agency [16].

3.3.1. Carbon Pricing Mechanisms

Carbon pricing elevates the comparative advantage of nuclear cogeneration over fossil fuel alternatives by internalizing avoided emissions. This relationship is quantified as:

$$\Delta NPV = \sum_{t=1}^{T} \frac{C_{avoid,t} P_{CO_2,t}}{(1+r)^t} \tag{21}$$

where $C_{avoided,t}$ represents avoided CO_2 emissions at time t and the unit is (t/y), $P_{CO2,t}$ denotes the carbon price, and r is the discount rate.

3.3.2. Value-Added Tax Exemption

VAT exemptions directly reduce the levelized cost by excluding non-electric outputs from taxation. The fiscal impact is expressed as:

$$LCOH_{VAT0} = LCOH(1 - \tau_{VAT}) \tag{22}$$

where τ_{VAT} is the VAT rate.

3.3.3. Subsidized Loans

Subsidized loans lower capital financing costs, enhancing project internal rates of return (IRR). The adjusted interest expense is modeled as:

$$I_{subsidized} = I_{market}(1 - s_{loan}) \tag{23}$$

where I_{market} is the market interest rate, and s_{loan} is the subsidy fraction.

4. Sector-Specific Economic Analyses of Nuclear Cogeneration

This section provides a comparative economic analysis of nuclear cogeneration across four key sectors: district heating systems, industrial process heat applications, hydrogen production, and desalination. Results are benchmarked against fossil fuel-based alternatives, with key metrics including levelized costs, capital expenditure (CAPEX), operational expenditure (OPEX), and CO_2 savings.

4.1. District Heating Systems

Nuclear-powered district heating has emerged as a cost-effective pathway for decarbonizing urban heat supply, with regional implementation models reflecting distinct economic and policy landscapes. In China, the Haiyang NHR-5 low-temperature reactor provides heating services for 450,000 square meters of urban infrastructure at USD 40 per megawatt-hour, supported by a 13% value-added tax exemption and state-funded thermal grid expansions [34]. By contrast, Russia's centralized nuclear heating model faces economic challenges, with production costs of USD 50–60 per megawatt-hour competing against subsidized natural gas prices of USD 30–45 per megawatt-hour, underscoring the necessity of policy realignment to enhance competitiveness.

Key economic viability thresholds for nuclear district heating are closely tied to regional energy market dynamics. In the European Union, breakeven natural gas prices for nuclear heat adoption range from USD 8 to USD 10 per million British thermal units (MMBtu) [74], a threshold surpassed during the 2023 price peak of USD 32 per MMBtu. Carbon pricing mechanisms further amplify financial returns, with each EUR 10-per-ton increase in CO_2 prices elevating project-specific internal rates of return (IRR) by 1.2%.

Retrofit costs for integrating nuclear reactors with district heating networks depend critically on geographic proximity. For instance, pipeline infrastructure spanning 5 km requires an investment of EUR 15 million, though existing nuclear facilities reduce capital expenditure (CAPEX) by repurposing turbine bypass systems and steam extraction points. Reported CO_2 savings of 0.15–0.25 metric tons per megawatt-hour assume the displacement of coal or natural gas boilers, with lifecycle emissions accounting for fuel extraction, transportation, and combustion phases [75]. These metrics position nuclear cogeneration as a scalable solution for urban decarbonization, contingent on region-specific policy and market frameworks.

4.2. Industrial Process Heat Applications

Nuclear cogeneration technologies are increasingly deployed to decarbonize energy-intensive industrial processes, offering both economic and operational advantages. In the oil sands sector, SMRs achieve an IRR of 9–11% when coupled with carbon credits priced at USD 50 per ton of CO_2 [39,76]. For steel production, China's Shidaowan high-temperature gas-cooled reactor (HTGR) enables a hydrogen-based direct reduction in iron ore, reducing fuel costs by 38% compared to conventional coal-fired processes [77]. In chemical synthesis, Terrestrial Energy's integral molten salt reactor (IMSR) integrated with methanol production systems extends catalyst lifespans by a factor of 1.8 through stable thermal output, minimizing downtime and maintenance costs [64].

These innovations align with global decarbonization imperatives. Supercritical water-cooled reactors (SCWRs) [78] can supply 550 °C steam for bitumen extraction, displacing natural gas consumption by 40%, while Japan's HTGRs achieve 40–50% thermal efficiency in co-delivering hydrogen and steam for steelmaking and ammonia synthesis [79]. Such systems underscore nuclear cogeneration's potential to decarbonize hard-to-abate industries while maintaining economic viability under carbon pricing frameworks.

4.3. Hydrogen Economy Synergies

Hydrogen production pathways via nuclear cogeneration demonstrate divergent efficiencies, cost structures, and carbon breakeven thresholds. High-temperature steam electrolysis (HTSE) achieves a system efficiency of 55% [80], yielding a levelized cost of hydrogen ($LCOH_2$) of between USD 3.2 and USD 4.5 per kilogram, contingent on carbon prices exceeding USD 80–90 per ton of CO_2 to achieve parity with conventional fossil-derived hydrogen. In contrast, sulfur–iodine thermochemical cycles operate at 48% efficiency, producing hydrogen at USD 4.5–5.8 per kilogram, with carbon breakeven thresholds rising to USD 100–120 per ton of CO_2 due to the higher capital intensity. Steam methane reforming, despite its superior 75% efficiency, incurs an additional USD 30 per ton of CO_2 for carbon capture and storage (CCS), elevating its $LCOH_2$ to USD 1.8–2.5 per kilogram while remaining carbon-intensive without full CCS deployment.

Policy frameworks are critical in accelerating market adoption of nuclear-driven hydrogen. The European Union's Hydrogen Quota Directive mandates that 10% of industrial hydrogen demand be met by low-carbon sources by 2030 [81], establishing a projected USD 12 billion annual revenue pool for nuclear and renewable hydrogen producers. These measures synergize with carbon pricing regimes exceeding USD 50 per ton of CO_2, under which nuclear cogeneration emerges as a cost-competitive alternative to fossil-based hydrogen, particularly in jurisdictions prioritizing decarbonization of heavy industries and chemical synthesis sectors.

4.4. Desalination Economics

Hybrid nuclear–desalination systems demonstrate significant cost efficiencies compared to conventional standalone facilities. The Jubail desalination plant in Saudi Arabia, integrated with a nuclear power plant, achieves a freshwater production cost of USD 0.90 per cubic meter, a 25% reduction from the USD 1.20 per cubic meter typical of isolated systems [82]. This cost advantage stems from shared infrastructure, particularly optimized cooling systems that minimize thermal energy losses. Similarly, China's Hongyanhe Nuclear Power Plant employs a thermal–membrane hybrid configuration, lowering specific energy consumption to 2.1 kilowatt-hours per cubic meter—a 40% improvement over traditional thermal desalination methods [83].

In addition to cost efficiency, brine monetization strategies enhance the economic viability of nuclear-powered desalination. Pilot projects in Chile have demonstrated the

feasibility of extracting high-purity lithium from desalination brine, generating incremental revenue of USD 0.30 per cubic meter [84]. In the United Arab Emirates, the Barakah Nuclear Power Plant offsets 30% of its desalination operational costs through the recovery and commercialization of magnesium and other minerals from brine byproducts [66]. These initiatives not only reduce net water production costs but also align with circular economy principles by transforming waste streams into valuable resources.

5. Market Dynamics and Policy Drivers

5.1. Regulatory Frameworks and Safety Paradigms

Nuclear cogeneration faces a fragmented regulatory landscape, with safety standards and liability regimes shaping market entry barriers. Ref. [85] mandates dual-layer containment for reactors supplying industrial heat, adding 12–18% to capital costs for high-temperature applications like hydrogen production. In contrast, China's Nuclear Energy Law (2023) adopts a risk-informed approach, allowing HTGRs to share safety systems with adjacent chemical plants if probabilistic risk assessments (PRAs) show a core damage frequency of less than 1×10^{-7}. Ref. [16] imposes strict liability caps, creating divergent insurance markets. For example, Canada's oil sands SMR projects leverage the Nuclear Liability Act's "channelings" principle to limit operator liability, reducing insurance premiums by 30% compared to EU counterparts.

5.2. Carbon Pricing and Emission Trading Mechanisms

Carbon pricing stands as the foremost policy instrument for enhancing the competitiveness of nuclear cogeneration by integrating the external costs of carbon emissions into economic decision-making. The European Union's Emissions Trading System [86], with carbon prices anticipated to reach EUR 105 per metric ton of CO_2 by 2025, enhances the financial viability of nuclear-powered district heating systems [87]. This pricing framework increases the net present value of such projects by 25–40% compared to fossil fuel-dependent alternatives. In parallel, China's national carbon market, operating at a lower price range of USD 28 per ton of CO_2 [88], primarily drives decarbonization efforts in hydrogen production and steel manufacturing sectors, aligning with its coal-intensive energy infrastructure.

Cross-sectoral evaluations highlight distinct regional carbon price thresholds required to achieve economic parity, as shown in Table 6. For district heating systems, the breakeven carbon price in the European Union approximates EUR 50 per ton of CO_2 [89], while the threshold in China is substantially lower, at USD 35 per ton of CO_2 [90,91]. This divergence reflects differing regional energy market structures, notably the prevalence of natural gas in Europe versus coal-dominated systems in China. In hydrogen production, thermochemical cycles employing high-temperature gas-cooled reactor technology necessitate carbon prices of USD 80–90 per ton to surpass fossil-based hydrogen economically [92]. By contrast, hybrid systems combining steam methane reforming with electrolysis attain feasibility at USD 60 per ton of CO_2 due to higher operational efficiencies [93].

Table 6. Carbon prices and key sectors in different regions.

Region	Carbon Price	Breakeven Threshold	Key Sector
EU	EUR 105/tCO_2 (2025)	EUR 50/tCO_2 (district heating)	District heating
China	USD 28/tCO_2	USD 35/tCO_2 (district heating)	Hydrogen/steel
Canada	Multi-credit	USD 80–90/tCO_2 (HTGR hydrogen)	Industrial hydrogen

A novel policy innovation, the Greenhouse Gas Credit Stacking mechanism, tested in Alberta, Canada, further strengthens nuclear cogeneration's financial attractiveness [94].

This mechanism permits the aggregation and monetization of multiple environmental credits, including CO_2, sulfur oxides, and nitrogen oxides, thereby augmenting project-specific internal rates of return by 4–6 percentage points. Such integrated credit systems not only address climate objectives but also improve air quality outcomes, illustrating the multifunctional policy potential in advancing capital-intensive, low-carbon infrastructure.

5.3. Subsidies and Tax Incentives

5.3.1. Direct Subsidies

Direct subsidies serve as a critical financial mechanism to mitigate the substantial capital expenditures inherent in deploying nuclear cogeneration infrastructure, as shown in Table 7. The European Union's Innovation Fund has committed EUR 4 billion over the 2021–2030 period to advance nuclear–renewable hybrid energy systems [95], specifically targeting thermal energy storage integration for molten salt reactors. By subsidizing 40% of these integration costs, the fund enables the simultaneous production of heat and electricity, enhancing operational flexibility and grid resilience. In China, a 13% exemption on value-added tax for non-electric outputs—such as heat and hydrogen—has reduced the levelized cost of heat by USD 8–12 per megawatt-hour [96]. This policy directly lowers energy costs for industrial consumers while incentivizing the adoption of low-carbon heat sources. Collectively, such subsidies address the financial risks of nuclear cogeneration deployment, particularly in regions where carbon pricing mechanisms remain nascent or underdeveloped.

Table 7. Subsidy programs in different regions.

Region	Subsidy Program	Funding/Coverage	Target Technology
EU	Innovation fund (N-RHES)	EUR 4B (2021–2030), 40% TES	Molten salt reactors
China	VAT exemption	13% tax relief on outputs	HTR-PM reactors

5.3.2. Tax Credits

Tax credits provide long-term revenue certainty for nuclear cogeneration projects by reducing operational cost burdens, as shown in Table 8. The U.S. 45X tax credit offers USD 3/kg for clean hydrogen produced via nuclear energy, bridging 30% of the cost gap with fossil-based "grey" hydrogen and accelerating HTGR deployments in hydrogen hubs [97]. In France, a heat premium of EUR 18/MWh, indexed to natural gas prices [98], stabilizes revenue streams for nuclear-sourced district heating, ensuring profitability even during energy price volatility. These instruments are particularly effective in liberalized markets where price fluctuations deter private investment.

Table 8. Tax credits in different regions.

Region	Tax Credit	Value	Target Output
U.S.	45X clean hydrogen credit	USD 3/kg for nuclear hydrogen	Industrial hydrogen
France	Heat premium	EUR 18/MWh (gas-indexed)	District heating

6. Future Prospects

Generation IV (Gen-IV) nuclear systems can achieve 40–50% thermal–electric efficiencies, with inherent safety features [57]. Gen-IV nuclear reactors represent a paradigm shift in nuclear technology, designed to address sustainability, safety, non-proliferation, and economic competitiveness. The Generation IV International Forum (GIF) has prioritized six systems for development, as shown in Table 9.

Table 9. Key cogeneration applications of Generation IV (Gen-IV) nuclear reactors.

Reactor Type	Coolant	Core Outlet Temperature Range (°C)	Key Cogeneration Applications
VHTR	Helium	750–1000	Hydrogen, ammonia, steelmaking
SFR	Sodium	500–550	Desalination, synthetic fuels
MSR	Fluoride	700–800	Hydrogen, chemical synthesis
GFR	Helium	850–950	Industrial process heat
LFR	Lead	480–800	District heating, desalination
SCWR	Water	374–625	High-efficiency power + heat

Current research and development efforts focus on integrating Generation IV reactors with high-temperature industrial processes and hybrid energy systems. In the realm of hydrogen production, very-high-temperature reactor (VHTR) technology has shown promise. Japan's high-temperature engineering test reactor (HTTR) has demonstrated the capability to co-produce hydrogen at a rate of 30% via sulfur–iodine cycles at temperatures of 950 °C [99]. A reactor with a thermal power of 1000 MWth could potentially produce 60,000 kg of hydrogen per day. Additionally, sodium-cooled fast reactor (SFR) technology is being explored. Russia's BN-1200 reactor incorporates sodium heat exchangers to produce high-purity hydrogen at 550 °C, with projected costs ranging from USD 2.5 to 3.0 per kilogram, which is significantly lower than the USD 4–6 per kilogram associated with electrolysis [17,32].

In terms of desalination and district heating applications, lead-cooled fast reactor (LFR) technology is being investigated. Europe aims to couple lead-cooled reactors with multi-effect distillation (MED) systems. This integration is expected to produce 120,000 cubic meters of freshwater per day at a cost of USD 0.7–1.0 per cubic meter, which is approximately 30% cheaper than fossil-based systems [100]. Meanwhile, molten salt reactor (MSR) technology is also being developed. Terrestrial Energy's integral molten salt reactor (IMSR) [64] is designed to supply 600 MWth for district heating in Canada, with the potential to reduce carbon emissions by 85% compared to traditional gas boilers.

Furthermore, the integration of thermal storage systems with Generation IV reactors is being explored to enhance the flexibility and efficiency of hybrid energy systems. A notable example is MIT's Gen-IV/solar hybrid system, which utilizes molten salt storage capable of providing 12–24 h of thermal energy storage. This integration helps balance grid demand and can increase capacity factors to approximately 90%. The cases currently under study are shown in Table 10

Table 10. Gen-IV nuclear cogeneration cases.

Project	Country	Reactor Type	Output (MWth)	Application
HTTR	Japan	VHTR	30	Hydrogen production
BN-1200	Russia	SFR	600	Hydrogen/desalination
ELFR	EU	LFR	300	Desalination
IMSR	Canada	MSR	600	District heating

7. Conclusions

Nuclear cogeneration, as a dual-output energy system, represents a paradigm shift in addressing the dual challenges of energy security and decarbonization. This review synthesizes advancements in technological stratification, economic modeling, and sectoral practices to establish its viability as a cornerstone of low-carbon energy transitions. The findings underscore the critical interplay between reactor design, hybrid system integra-

tion, and policy alignment in unlocking the full potential of nuclear cogeneration across diverse applications.

The temperature-dependent stratification of nuclear cogeneration systems highlights their adaptability to sector-specific demands. Low-temperature applications (<250 °C), such as district heating and desalination, leverage mature light water reactor (LWR) technologies to achieve thermal efficiencies exceeding 80%. These systems demonstrate near-term scalability but require significant retrofitting investments (EUR 15–30 million for pipeline infrastructure) and policy support to offset upfront costs. Medium-temperature systems (250–550 °C), exemplified by Canada's SMRs delivering 280 °C steam for oil sands processing, bridge the gap between industrial decarbonization and operational reliability, reducing emissions by 30% per barrel. High-temperature applications (>550 °C), such as hydrogen production via thermochemical cycles (Japan's GTHTR300C at USD 3–5/kg H_2) and petrochemical heat supply (China's HTR-PM), necessitate advanced reactors (HTGRs, MSRs) to overcome Carnot limitations and achieve system efficiencies of up to 88%.

Economic analyses reveal that cost allocation methodologies significantly influence project feasibility. Exergy-based approaches, which account for thermodynamic quality, outperform energy-equivalent methods in high-temperature applications, reducing levelized costs by 18% when integrated with thermal energy storage (TES). Carbon pricing emerges as a pivotal driver, with EU prices (EUR 105/tCO_2 by 2025) elevating district heating project NPVs by 25–40% and breakeven thresholds for hydrogen production at USD 80–90/tCO_2. Policy instruments such as VAT exemptions (e.g., China's 13% tax relief) and subsidized loans (e.g., the U.S.'s 45X hydrogen credits) further enhance IRR by 4–6 percentage points. Hybrid nuclear–renewable systems, combining molten salt reactors with solar thermal or rock-bed TES, stabilize energy supply and reduce the levelized cost of heat (LCOH) by 18%, demonstrating the economic merits of multi-energy integration.

In the future, Gen-IV reactors will enable transformative cogeneration applications. While FOAK costs remain high, economies of scale and hybrid system integration promise 20–30% cost reductions by 2040.

Author Contributions: Methodology, G.J.; validation, G.Z.; formal analysis, J.W.; investigation, J.T.; resources, G.Z.; data curation, Y.Z.; writing—original draft preparation, G.J.; writing—review and editing, Y.M.; visualization, Y.D.; supervision, J.T.; funding acquisition, J.W. All authors have read and agreed to the published version of the manuscript.

Funding: This research was funded by the [National Natural Science Foundation of China] (Grant No. 12475185) and the [Shanghai Municipal Natural Science Foundation] (Grant No. 24ZR1478500).

Data Availability Statement: The authors do not have permission to share data.

Conflicts of Interest: The authors declare that they have no known competing financial interests or personal relationships that could have appeared to influence the work reported in this paper.

Nomenclature

LWR	light water reactor
HTGR	high-temperature gas-cooled reactor
MSR	molten salt reactor
VAT	value-added tax
NPP	nuclear power plant
CHP	combined heat and power
TES	thermal energy storage
BWR	boiling water reactor
VHTR	very-high-temperature reactor

PHWR	pressurized heavy water reactor
LWGR	light water graphite reactor
LCOE	levelized cost of electricity
LCONE	levelized cost of non-electricity
NPV	net present value
IRR	internal rate of return
LFR	lead-cooled fast reactor
HT	high temperature
CRF	capital recovery factor
SFF	sinking fund factor

References

1. Shcheklein, S.E.; Tashlykov, O.L.; Dubinin, A.M. Improving the energy efficiency of NPP. *Nucl. Energy Technol.* **2016**, *2*, 30–36. [CrossRef]
2. Congedo, T.; Lahoda, E.; Matzie, R.; Task, K. The Nuclear Industry. In *Handbook of Industrial Chemistry and Biotechnology*; Kent, J.A., Ed.; Springer: Boston, MA, USA, 2012; pp. 829–874.
3. Zakharikhina, L.V.; Lesnikova, P.S.; Kerimzade, V.V. Exploring secondary contamination in river and spring waters: A novel phenomenon arising from seawater intrusion into deep coastal aquifers. *Mar. Pollut. Bull.* **2025**, *211*, 117364. [CrossRef] [PubMed]
4. Chen, C.-T.; Jan, S.; Chen, M.-H.; Liu, L.-L.; Huang, J.-F.; Yang, Y.-J. Far-Field Influences Shadow the Effects of a Nuclear Power Plant's Discharges in a Semi-Enclosed Bay. *Sustainability* **2023**, *15*, 9092. [CrossRef]
5. Guimarães, L.S.F.; de Carvalho-Junior, L.; Façanha, G.L.; Resende, N.d.S.; Neves, L.M.; Cardoso, S.J. Meta-analysis of the thermal pollution caused by coastal nuclear power plants and its effects on marine biodiversity. *Mar. Pollut. Bull.* **2023**, *195*, 115452. [CrossRef]
6. Sukhorukov, Y.G.; Smolkin, Y.V.; Kazarov, G.I.; Kulakov, E.N.; Kondurov, E.P.; Popov, A.V. Directions for Increasing Thermal Efficiency of an NPP with PWR. *Therm. Eng.* **2024**, *71*, 583–590. [CrossRef]
7. Novotný, V.; Kim, J.; Cho, S.-B.; Saeed, R.M. Nuclear—Thermal energy storage configurations for industrial combined heat and power supply—Conceptual and thermodynamic study with high temperature gas-cooled reactor. *Energy* **2025**, *322*, 135544. [CrossRef]
8. Khan, S.U.-D.; Khan, S.U.-D.; Danish, S.N.; Orfi, J.; Rana, U.A.; Haider, S. Chapter 6—Nuclear Energy Powered Seawater Desalination. In *Renewable Energy Powered Desalination Handbook*; Gude, V.G., Ed.; Butterworth-Heinemann: Oxford, UK, 2018; pp. 225–264.
9. Ding, L.; Zhang, R.; Wang, C.; Xing, J. Research on Nuclear Seawater Desalination Technology Based on Small Modular Reactor ACP100. In Proceedings of the 23rd Pacific Basin Nuclear Conference, Beijing&Chengdu, China, 1–4 November 2022; Spring: Singapore, 2023; Volume 3, pp. 853–866.
10. IAEA. *New Technologies for Seawater Desalination Using Nuclear Energy*; International Atomic Energy Agency: Vienna, Austria, 2015.
11. Leurent, M.; Da Costa, P.; Rämä, M.; Persson, U.; Jasserand, F. Cost-benefit analysis of district heating systems using heat from nuclear plants in seven European countries. *Energy* **2018**, *149*, 454–472. [CrossRef]
12. Samoilov, O.B.; Kurachenkov, A.V. Nuclear district heating plants AST-500. Present status and prospects for future in Russia. *Nucl. Eng. Des.* **1997**, *173*, 109–117. [CrossRef]
13. Angulo, C.; Bogusch, E.; Bredimas, A.; Delannay, N.; Viala, C.; Ruer, J.; Muguerra, P.; Sibaud, E.; Chauvet, V.; Hittner, D.; et al. EUROPAIRS: The European project on coupling of High Temperature Reactors with industrial processes. *Nucl. Eng. Des.* **2012**, *251*, 30–37. [CrossRef]
14. Hampe, J.; Madlener, R. *Economics of High-Temperature Nuclear Reactors for Industrial Cogeneration*; E.ON Energy Research Center, Future Energy Consumer Needs and Behavior (FCN): Aachen, Germany, 2012.
15. Ruth, M.F.; Zinaman, O.R.; Antkowiak, M.; Boardman, R.D.; Cherry, R.S.; Bazilian, M.D. Nuclear-renewable hybrid energy systems: Opportunities, interconnections, and needs. *Energy Convers. Manag.* **2014**, *78*, 684–694. [CrossRef]
16. IAEA. *Guidance on Nuclear Energy Cogeneration*; International Atomic Energy Agency: Vienna, Austria, 2019.
17. NEA. *Beyond Electricity: The Economics of Nuclear Cogeneration*; Nuclear Energy Agency (NEA): Paris, France, 2022.
18. Dincer, I.; Bicer, Y. Chapter 5—Integration of nuclear energy systems for multigeneration. In *Integrated Energy Systems for Multigeneration*; Dincer, I., Bicer, Y., Eds.; Elsevier: Amsterdam, The Netherlands, 2020; pp. 223–285.
19. Choudhury, M.; Roy, P. Challenges with microplastic pollution in the regime of UN sustainable development goals. *World Dev. Sustain.* **2025**, *6*, 100216. [CrossRef]

20. Moeen, M.S.; Jupesta, J.; Hanaoka, T. Integrated energy planning: Review of global practices for energy security and Paris Agreement implementation in Pakistan. *Energy Nexus* **2025**, *18*, 100413. [CrossRef]
21. Jasserand, F.; Devezeaux de Lavergne, J.-G. Initial economic appraisal of nuclear district heating in France. *EPJ—Nucl. Sci. Technol.* **2016**, *2*, 39. [CrossRef]
22. Lee, S.W.; Kim, D.; Seo, J.; Jo, H. Economic evaluations of hydrogen production and storage systems coupled with high-temperature gas-cooled reactors. *Int. J. Hydrogen Energy* **2025**, *124*, 191–203. [CrossRef]
23. Huang, J.-L.; Jia, G.-B.; Han, L.-F.; Liu, W.-Q.; Huang, L.; Yang, Z.-H. Dynamic simulation analysis of molten salt reactor-coupled air–steam combined cycle power generation system. *Nucl. Sci. Tech.* **2024**, *35*, 30. [CrossRef]
24. Sato, H.; Yan, X.L.; Tachibana, Y.; Kunitomi, K. GTHTR300—A nuclear power plant design with 50% generating efficiency. *Nucl. Eng. Des.* **2014**, *275*, 190–196. [CrossRef]
25. Peng, C.; Zhang, H.; Wu, Y.; Guo, J.; Peng, W.; Zhang, P.; Li, F. Assessment of hydrogen leakage hazards in VHTR-based nuclear hydrogen production systems: A variable pressure analysis model. *Int. J. Hydrogen Energy* **2025**, *128*, 223–235. [CrossRef]
26. Mignacca, B.; Locatelli, G. Economics and finance of Molten Salt Reactors. *Prog. Nucl. Energy* **2020**, *129*, 103503. [CrossRef]
27. Yang, Q.; Zheng, Y.; Wu, H. Advancements and challenges in small modular lead/lead bismuth eutectic cooled fast reactors: A 30-year overview. *Ann. Nucl. Energy* **2025**, *218*, 111434. [CrossRef]
28. Lindroos, T.; Pursiheimo, E.; Sahlberg, V.; Tulkki, V. A techno-economic assessment of NuScale and DHR-400 reactors in a district heating and cooling grid. *Energy Sources Part B-Econ. Plan. Policy* **2019**, *14*, 13–24. [CrossRef]
29. Yoo, Y.; Arunachalam, M.; Elmakki, T.; Al-Ghamdi, A.S.; Bassi, H.M.; Mohammed, A.M.; Ryu, S.; Yong, S.; Shon, H.K.; Park, H.; et al. Evaluating the economic and environmental viability of small modular reactor (SMR)-powered desalination technologies against renewable energy systems. *Desalination* **2025**, *602*, 118624. [CrossRef]
30. IAEA. *Opportunities for Cogeneration with Nuclear Energy*; International Atomic Energy Agency: Vienna, Austria, 2017.
31. Thilagam, L.; Mohapatra, D.K. Preliminary neutronics analysis for generation III+ VVER design—VVER-1200. *Nucl. Part. Phys. Proc.* **2023**, *341*, 98–103. [CrossRef]
32. Vasilyev, B.A.; Vasyaev, A.V.; Gusev, D.V.; Marova, E.V.; Staroverov, A.I.; Shepelev, S.F. Current status of BN-1200M reactor plant design. *Nucl. Eng. Des.* **2021**, *382*, 111384. [CrossRef]
33. Kalyakin, S.G.; Kozlov, F.A.; Sorokin, A.P.; Bogoslovskaya, G.P.; Ivanov, A.P.; Konovalov, M.A.; Morozov, A.V.; Stogov, V.Y. Investigations for the substantiation of high-temperature nuclear power generation technology using fast sodium-cooled reactor for hydrogen production and other innovative applications (Part 1). *Nucl. Energy Technol.* **2016**, *2*, 282–286. [CrossRef]
34. Li, Y.; Chen, C.; Hu, J.; Su, J.; Liu, H. Analysis of Current Status and Development Trend of Nuclear District Heating. In Proceedings of the 23rd Pacific Basin Nuclear Conference, Volume 3, Beijing&Chengdu, China, 1–4 November 2022; Spring: Singapore, 2023; pp. 301–307.
35. Weiqi, L.; Jinshi, W.; Kai, X.; Zhiyong, S.; Xingmin, L.; Gen, L.; Junjie, Y. Capacity Configuration and Operation Optimization of a Low-Temperature Reactor Nuclear Heating System with Heat Storage. *Nucl. Power Eng.* **2024**, *45*, 213–220.
36. Liu, W.; Zhao, Q.; Sun, Z.; Liu, X.; Li, G.; Yan, J.; Wang, J. Economic optimization and thermodynamic analysis of a novel nuclear district cooling system. *Appl. Therm. Eng.* **2024**, *247*, 123042. [CrossRef]
37. Kim, K.; Kim, D.; Ju, H. *Nuclear Power Plant Cogeneration System, Has District Heating Heat Exchanger for Producing Hot Water, and Thermal Storage Tank for Storing Thermal Energy by Using Steam Extracted from Turbine*; Korea Hydro & Nuclear Power Co., Ltd. (Kepc-C): Gyeongju, Republic of Korea, 2025.
38. Sundarrajan, P.; Thakur, J.; Meha, D. Harnessing hydrogen and thermal energy storage: Sweden's path to a 100 % renewable energy system by 2045. *Renew. Sustain. Energy Rev.* **2025**, *210*, 115041. [CrossRef]
39. Sanongboon, P.; Pettigrew, T.; Moore, M. Techno-economic analysis of small modular reactor for oil sands extraction and upgrading in Canada. *Nucl. Eng. Des.* **2024**, *425*, 113325. [CrossRef]
40. Xing, J.; Song, D.; Wu, Y. HPR1000: Advanced Pressurized Water Reactor with Active and Passive Safety. *Engineering* **2016**, *2*, 79–87. [CrossRef]
41. IAEA. *Nuclear–Renewable Hybrid Energy Systems for Decarbonized Energy Production and Cogeneration*; International Atomic Energy Agency: Vienna, Austria, 2019.
42. Kang, S.; Yim, M. Coupled system model analysis for a small modular reactor cogeneration (combined heat and power) application. *Energy* **2023**, *262*, 125481. [CrossRef]
43. Lin, N.; Xu, L. Navigating the Implementation of Tax Credits for Natural-Gas-Based Low-Carbon-Intensity Hydrogen Projects. *Energies* **2024**, *17*, 1604. [CrossRef]
44. Iakovleva, M.; Rayner, J. Accelerating the deployment of SMRs in Canada: The importance of intermediaries. *Environ. Innov. Soc. Transit.* **2024**, *53*, 100918. [CrossRef]
45. Dong, Z.; Zhang, Z.; Dong, Y.; Shi, L.; Huang, X.; Zhu, Y.; Jiang, D. Testing the feasibility of multi-modular design in an HTR-PM nuclear plant. *Nat. Commun.* **2025**, *16*, 2778. [CrossRef]
46. Mansouri, N.Y.; Ghoniem, A.F. Does nuclear desalination make sense for Saudi Arabia? *Desalination* **2017**, *406*, 37–43. [CrossRef]

47. Ahmad, A.; Ramana, M.V. Too costly to matter: Economics of nuclear power for Saudi Arabia. *Energy* **2014**, *69*, 682–694. [CrossRef]
48. Sawicki, J.; Brett, M. Mossbauer Study of Corrosion Products from a CANDU Secondary System. *Nucl. Instrum. Methods Phys. Res. Sect. B-Beam Interact. Mater. At.* **1993**, *76*, 254–257. [CrossRef]
49. Starkov, S.O.; Lavrenkov, Y.N. Prediction of the moderator temperature field in a heavy water reactor based on a cellular neural network. *Nucl. Energy Technol.* **2017**, *3*, 133–140. [CrossRef]
50. Yan, X.; Sato, H.; Sumita, J.; Nomoto, Y.; Horii, S.; Imai, Y.; Kasahara, S.; Suzuki, K.; Iwatsuki, J.; Terada, A.; et al. Design of HTTR-GT/H_2 test plant. *Nucl. Eng. Des.* **2018**, *329*, 223–233. [CrossRef]
51. Kunitomi, K.; Yan, X.; Nishihara, T.; Sakaba, N.; Mouri, T. Jaea's VHTR for hydrogen and electricity cogeneration: GTHTR300C. *Nucl. Eng. Technol.* **2007**, *39*, 9–20. [CrossRef]
52. 2—Features of a PWR plant. In *Pressurized Water Reactors*; Mimaki, H., Kanzaki, Y., Yamamoto, T., Eds.; Elsevier: Amsterdam, The Netherlands, 2024; pp. 43–262.
53. Nishio, H.; Kitani, T.; Kurashige, T. 5—Advanced PWRs. In *Pressurized Water Reactors*; Mimaki, H., Kanzaki, Y., Yamamoto, T., Eds.; Elsevier: Amsterdam, The Netherlands, 2024; pp. 347–402.
54. Matsuura, M.; Shirahama, H.; Kawai, H.; Suzuki, H.; Katayama, Y.; Ikeda, H. 2—Features of BWR plant. In *Boiling Water Reactors*; Nishida, K., Morooka, S., Mori, M., Koizumi, Y., Eds.; Elsevier: Amsterdam, The Netherlands, 2023; Volume 4, pp. 59–165.
55. Duffey, R.B.; Pioro, I.L.; Pioro, R. 1—Introduction. World energy production and the contribution of PHWRs. In *Pressurized Heavy Water Reactors*; Riznic, J.R., Ed.; Elsevier: Amsterdam, The Netherlands, 2022; Volume 7, pp. 1–44.
56. Filburn, T.; Bullard, S. Russian Reactor Design History. In *Three Mile Island, Chernobyl and Fukushima: Curse of the Nuclear Genie*; Springer International Publishing: Cham, Switzerland, 2016; pp. 43–53.
57. Locatelli, G.; Mancini, M.; Todeschini, N. Generation IV nuclear reactors: Current status and future prospects. *Energy Policy* **2013**, *61*, 1503–1520. [CrossRef]
58. Ingersoll, D.; Houghton, Z.; Bromm, R.; Desportes, C. NuScale small modular reactor for Co-generation of electricity and water. *Desalination* **2014**, *340*, 84–93. [CrossRef]
59. Squarer, D.; Schulenberg, T.; Struwe, D.; Oka, Y.; Bittermann, D.; Aksan, N.; Maraczy, C.; Kyrki-Rajamäki, R.; Souyri, A.; Dumaz, P. High performance light water reactor. *Nucl. Eng. Des.* **2003**, *221*, 167–180. [CrossRef]
60. Kraemer, J.; Bauer, H. New Russian reactor concepts. *Atw-Int. Z. Kernenerg.* **1996**, *41*, 237–243.
61. Khamis, I.; Kavvadias, K.C.; Sánchez-Cervera, I.G. Nuclear desalination: A viable option of the future based on existing experience. *Desalination Water Treat.* **2011**, *33*, 316–322. [CrossRef]
62. Khalid, F.; Dincer, I.; Rosen, M.A. Comparative assessment of CANDU 6 and Sodium-cooled Fast Reactors for nuclear desalination. *Desalination* **2016**, *379*, 182–192. [CrossRef]
63. Zohuri, B. Nuclear Hydrogen Production Plants. In *Hydrogen Energy: Challenges and Solutions for a Cleaner Future*; Springer International Publishing: Cham, Switzerland, 2019; pp. 185–227.
64. LeBlanc, D.; Rodenburg, C. 18—Integral molten salt reactor. In *Molten Salt Reactors and Thorium Energy*; Dolan, T.J., Ed.; Woodhead Publishing: Cambridge, UK, 2017; pp. 541–556.
65. Johar, D.; Sharma, D.; Soni, S. Comparative studies on micro cogeneration, micro cogeneration with thermal energy storage and micro trigeneration with thermal energy storage system using same power plant. *Energy Convers. Manag.* **2020**, *220*, 113082. [CrossRef]
66. Al Rashdi, M.R.; Alaabed, S.; El Tokhi, M.; Howari, F.M.; El Mowafi, W.; Arabi, A.A. Distribution of heavy metals around the Barakah nuclear power plant in the United Arab Emirates. *Environ. Sci. Pollut. Res.* **2017**, *24*, 19835–19851. [CrossRef]
67. Moore, M.; Korinny, A.; Shropshire, D.; Sadhankar, R. Benchmarking of nuclear economics tools. *Ann. Nucl. Energy* **2017**, *103*, 122–129. [CrossRef]
68. Geissmann, T. A probabilistic approach to the computation of the levelized cost of electricity. *Energy* **2017**, *124*, 372–381. [CrossRef]
69. Stoiljkovic, V. Net present value analysis-Comparing engineering projects by financial return. *IEEE Potentials* **2010**, *29*, 17–21. [CrossRef]
70. Barry, P.; Robison, L. Technical Note: Economic Rates of Return and Investment Analysis. *Eng. Econ.* **2014**, *59*, 231–236. [CrossRef]
71. Gupta, R.; Soini, M.; Patel, M.; Parra, D. Levelized cost of solar photovoltaics and wind supported by storage technologies to supply firm electricity. *J. Energy Storage* **2020**, *27*, 101027. [CrossRef]
72. Tariq, S.; Safder, U.; Yoo, C. Exergy-based weighted optimization and smart decision-making for renewable energy systems considering economics, reliability, risk, and environmental assessments. *Renew. Sustain. Energy Rev.* **2022**, *162*, 112445. [CrossRef]
73. Carlsson, J.; Shropshire, D.; van Heek, A.; Fütterer, M. Economic viability of small nuclear reactors in future European cogeneration markets. *Energy Policy* **2012**, *43*, 396–406. [CrossRef]
74. Correljé, A. The European Natural Gas Market. *Curr. Sustain./Renew. Energy Rep.* **2016**, *3*, 28–34. [CrossRef]
75. Yue, X.-L.; Gao, Q.-X. Contributions of natural systems and human activity to greenhouse gas emissions. *Adv. Clim. Change Res.* **2018**, *9*, 243–252. [CrossRef]

76. Ashoori, S.; Gates, I.D. Small modular nuclear reactors: A pathway to cost savings and environmental progress in SAGD operations. *Next Energy* **2024**, *4*, 100128. [CrossRef]
77. Zhang, Z.; Dong, Y.; Li, F.; Zhang, Z.; Wang, H.; Huang, X.; Li, H.; Liu, B.; Wu, X.; Wang, H.; et al. The Shandong Shidao Bay 200 MWe High-Temperature Gas-Cooled Reactor Pebble-Bed Module (HTR-PM) Demonstration Power Plant: An Engineering and Technological Innovation. *Engineering* **2016**, *2*, 112–118. [CrossRef]
78. Schulenberg, T.; Leung, L.K.H.; Oka, Y. Review of R&D for supercritical water cooled reactors. *Prog. Nucl. Energy* **2014**, *77*, 282–299.
79. Hada, K.; Shibata, T.; Nishihara, T.; Shiozawa, S. Universally applicable design concept of stably controlling an HTGR-hydrogen production system. *J. At. Energy Soc. Jpn.* **1996**, *38*, 834–844. [CrossRef]
80. Hino, R.; Miyamoto, Y. Preliminary Test of Hydrogen-Production by High-Temperature Electrolysis of Steam. *J. At. Energy Soc. Jpn.* **1993**, *35*, 546–548. [CrossRef]
81. Bleischwitz, R.; Bader, N. Policies for the transition towards a hydrogen economy: The EU case. *Energy Policy* **2010**, *38*, 5388–5398. [CrossRef]
82. Baig, M.B.; Al Kutbi, A.A. Design features of a 20 migd SWRO desalination plant, Al Jubail, Saudi Arabia. *Desalination* **1998**, *118*, 5–12. [CrossRef]
83. Yan, H.-m.; Cao, C.-y.; Bai, G.; Bai, W. *Seawater Desalination Technology Route and Analysis of Production Capacity for Large Commercial Nuclear Power Plant*; Spring: Singapore, 2017; pp. 865–872.
84. Shahmansouri, A.; Min, J.; Jin, L.; Bellona, C. Feasibility of extracting valuable minerals from desalination concentrate: A comprehensive literature review. *J. Clean. Prod.* **2015**, *100*, 4–16. [CrossRef]
85. Boev, B. Non-Electric Applications of Nuclear Energy—A Theoretical Overview and Socioeconomic Opportunities. 2023. Available online: https://www.researchgate.net/publication/374701541_NON-ELECTRIC_APPLICATIONS_OF_NUCLEAR_ENERGY_-_A_THEORETICAL_OVERVIEW_AND_SOCIOECONOMIC_OPPORTUNITIES (accessed on 28 May 2025).
86. Salant, S.W. What ails the European Union's emissions trading system? *J. Environ. Econ. Manag.* **2016**, *80*, 6–19. [CrossRef]
87. Schultz, E.; Swieringa, J. Catalysts for price discovery in the European Union Emissions Trading System. *J. Bank. Financ.* **2014**, *42*, 112–122. [CrossRef]
88. Weng, Q.; Xu, H. A review of China's carbon trading market. *Renew. Sustain. Energy Rev.* **2018**, *91*, 613–619. [CrossRef]
89. Brink, C.; Vollebergh, H.R.J.; van der Werf, E. Carbon pricing in the EU: Evaluation of different EU ETS reform options. *Energy Policy* **2016**, *97*, 603–617. [CrossRef]
90. Weng, Y.; Da, Z.; Lanlan, L.; and Zhang, X. A general equilibrium analysis of floor prices for China's national carbon emissions trading system. *Clim. Policy* **2018**, *18* (Suppl. S1), 60–70. [CrossRef]
91. Zhang, M.; Liu, Y.; Su, Y. Comparison of Carbon Emission Trading Schemes in the European Union and China. *Climate* **2017**, *5*, 70. [CrossRef]
92. Elder, R.; Allen, R. Nuclear heat for hydrogen production: Coupling a very high/high temperature reactor to a hydrogen production plant. *Prog. Nucl. Energy* **2009**, *51*, 500–525. [CrossRef]
93. Katebah, M.; Al-Rawashdeh, M.m.; Linke, P. Analysis of hydrogen production costs in Steam-Methane Reforming considering integration with electrolysis and CO2 capture. *Clean. Eng. Technol.* **2022**, *10*, 100552. [CrossRef]
94. Jordaan, S.M.; Romo-Rabago, E.; McLeary, R.; Reidy, L.; Nazari, J.; Herremans, I.M. The role of energy technology innovation in reducing greenhouse gas emissions: A case study of Canada. *Renew. Sustain. Energy Rev.* **2017**, *78*, 1397–1409. [CrossRef]
95. deLlano-Paz, F.; Calvo-Silvosa, A.; Iglesias Antelo, S.; Soares, I. The European low-carbon mix for 2030: The role of renewable energy sources in an environmentally and socially efficient approach. *Renew. Sustain. Energy Rev.* **2015**, *48*, 49–61. [CrossRef]
96. Zhang, Z.; Sun, Y. Economic potential of modular reactor nuclear power plants based on the Chinese HTR-PM project. *Nucl. Eng. Des.* **2007**, *237*, 2265–2274. [CrossRef]
97. Borenstein, S.; Davis, L.W. The Distributional Effects of US Clean Energy Tax Credits. *Tax Policy Econ.* **2016**, *30*, 191–234. [CrossRef]
98. Berry, A. The distributional effects of a carbon tax and its impact on fuel poverty: A microsimulation study in the French context. *Energy Policy* **2019**, *124*, 81–94. [CrossRef]
99. Miyamoto, Y.; Shiozawa, S.; Ogawa, M.; Hada, K.; Inagaki, Y.; Takeda, T.; Nishihara, T. Overview of hydrogen production program in HTTR. In Proceedings of the IAEA Technical Committee Meeting on High Temperature Gas Cooled Reactor Applications and Future Prospects, Petten, The Netherlands, 10–12 November 1997; pp. 121–131.
100. Chebac, R.; Cammi, A.; Ricotti, M.E.; Lorenzi, S.; Sadeghi, K.; Hadi Ghazaie, S.; Sokolova, E.; Fedorovich, E. ALFRED reactor and hybrid systems: A test case. *Ann. Nucl. Energy* **2023**, *191*, 109934. [CrossRef]

Disclaimer/Publisher's Note: The statements, opinions and data contained in all publications are solely those of the individual author(s) and contributor(s) and not of MDPI and/or the editor(s). MDPI and/or the editor(s) disclaim responsibility for any injury to people or property resulting from any ideas, methods, instructions or products referred to in the content.